Siegert-state expansion in the Kramers-Henneberger frame: Interference substructure of above-threshold ionization peaks in the stabilization regime

Koudai Toyota,[1] Oleg I. Tolstikhin,[2] Toru Morishita,[1] and Shinichi Watanabe[1]
[1]*Department of Applied Physics and Chemistry, University of Electro-Communications, 1-5-1, Chofu-ga-oka, Chofu-shi, Tokyo, Japan*
[2]*Russian Research Center "Kurchatov Institute," Kurchatov Square 1, Moscow 123182, Russia*
(Received 12 July 2007; published 17 October 2007)

The Siegert-state expansion approach is applied to the solution of the time-dependent Schrödinger equation describing a model one-dimensional laser-atom interaction problem in the Kramers-Henneberger frame. Our method is mathematically rigorous and numerically exact even though a very restricted spatial box is considered, since the use of Siegert states as a basis in the expansion eliminates unphysical reflections from the boundary of the box and the Kramers-Henneberger frame enables us to fully take the interaction with the laser field into account. The method is demonstrated by calculations of above-threshold ionization spectra generated by strong high-frequency laser pulses. We found an oscillating substructure of multiphoton peaks caused by an interference of photoelectron wave packets produced at different times during the pulse which becomes especially pronounced in the stabilization regime. An interpretation of this effect in terms of the high-frequency Floquet theory is given.

DOI: 10.1103/PhysRevA.76.043418 PACS number(s): 32.80.Rm, 31.15.−p, 31.70.Hq, 34.10.+x

I. INTRODUCTION

From the theoretical point of view, how to implement the numerical scheme to study a laser-atom interaction is a fundamental issue. Solving the time-dependent Schrödinger equation (TDSE) in the laboratory frame with absorbing boundary conditions in a large box is a widely used approach, see, e.g., Refs. [1–4]. However, this scheme substantially bears the following problems. First, the laboratory frame modifies the dynamics since the laser field must be eventually cut off beyond a finite box considered in the calculations. Second, the dynamics is disturbed also by the absorbing potential, whose effect is difficult to control and disentangle. Under the circumstances, Reed and Burnett [5] suggested to use the Kramers-Henneberger (KH) frame [6,7] instead of the laboratory frame. In the KH frame, the interaction with the laser field is represented by a quiver motion of the center of the atomic potential along a trajectory a classical electron would follow. Hence it is localized in a finite region of space where the atomic potential is effective. The electron moves freely once it leaves this interaction region. As was demonstrated in Ref. [5], this fact enables one to increase (approximately double) the length of a laser pulse that can be treated, because the calculations can be extended up to the moment when the electron returns to the interaction region after its reflection from the boundary of the box. Alternatively, one can reduce (approximately halve) the size of the box. In any case, a gain in the computational efficiency is achieved. The advantage of the KH frame is well recognized in [8,9]. In Ref. [5], zero boundary conditions were used. In this case, to calculate the spectrum the box must substantially exceed the interaction region, finiteness of the box obviously limits the high-energy extent of the spectrum obtained as well as its resolution. The gain from the use of the KH frame would be much more essential if one could reduce the size of the box to that of the interaction region. The absorbing boundary conditions may help to reach this goal, but if only the total ionization probability is needed. The true solution lies in correctly implementing the *outgoing-wave* boundary conditions. In this paper, we present a method in which only the interaction region is to be considered and, at the same time, which is capable of calculating spectra up to any desired energy and without any limitations on the resolution.

The idea consists in applying the recently developed Siegert-state expansion approach [10,11] to the solution of the TDSE in the KH frame. Siegert states (SSs) are the solutions to the stationary Schrödinger equation satisfying outgoing-wave boundary conditions. The corresponding eigenvalue problem was first considered by Siegert [12] for *s*-wave scattering in a finite range potential. SSs remained a formal object in scattering theory until Tolstikhin *et al.* [13–15] developed an algebraic formulation known as the theory of Siegert pseudostates (SPSs) which became a powerful tool in practical calculations. Recently, this formulation was supplemented by a discussion of the SPS perturbation theory [16]. More recently, it has been generalized to nonzero angular momenta [17]. In the stationary framework, SPSs have been employed, for example, for the calculation of resonances in three-body Coulomb systems [18–20]. Yoshida *et al.* [21] and Tanabe *et al.* [22] pioneered the applications of SPSs as a basis to treat time propagation of wave packets. The advantage of such a basis is that it does not produce an unphysical reflection at the boundary of the box because the outgoing-wave boundary conditions are satisfied. Subsequently, Santra *et al.* [23] following an earlier work [24] developed a rigorous formalism of the expansion in terms of SPSs for the case of a stationary Hamiltonian. Finally, Tolstikhin [10,11] has extended the method to time-dependent Hamiltonians, which made its applications to many nonstationary problems such as laser-atom interaction possible.

In the calculations reported in Ref. [11], a model one-dimensional atom in the laboratory frame was considered. In this paper, we consider the same problem in the KH frame. The SS expansion approach [10,11] enables us to solve the

TDSE avoiding unphysical reflections from the boundary of the box. The use of the KH frame guarantees that the interaction with the laser field is fully taken into account so long as the box is large enough to cover the interaction region. When these two elements are combined, the method is free from any approximations despite the use of a very restricted box size. But the main advantage of the method is its ability to produce accurate highly resolved spectra.

The paper is organized as follows. In Sec. II, basic equations of our approach are formulated. In Sec. III, the approach is applied to the calculations of above-threshold ionization (ATI) spectra [25]. First we revisit the model considered in Ref. [11]. The present calculations are essentially exact, because there is no need to cut off the laser field as it was the case in Ref. [11]. Then we discuss the same model, but for a much stronger laser field. An interesting interference substructure of ATI peaks generated by high-frequency pulses is found in the stabilization regime. Its interpretation in terms of an adiabatic version of the high-frequency Floquet theory [8,26] is given. The effect is demonstrated also by calculations for a model describing photodetachment of H^-. Section V concludes the paper.

II. THEORETICAL APPROACH

A. Time-dependent Schrödinger equation in the Kramers-Henneberger frame

We consider an electron in a model one-dimensional atom interacting with a laser pulse. Our starting point is the TDSE in the laboratory (L) frame in the length gauge (atomic units $\hbar=m=|e|=1$ are used throughout the paper, unless otherwise stated)

$$i\frac{\partial\psi_{\mathrm{L}}(x_{\mathrm{L}},t)}{\partial t}=\left[-\frac{1}{2}\frac{\partial^2}{\partial x_{\mathrm{L}}^2}+V(x_{\mathrm{L}})+F(t)x_{\mathrm{L}}\right]\psi_{\mathrm{L}}(x_{\mathrm{L}},t). \quad (1)$$

The atomic potential $V(x_{\mathrm{L}})$ is assumed to vanish beyond a finite interval $-X\leqslant x_{\mathrm{L}}\leqslant X$,

$$V(|x_{\mathrm{L}}|>X)=0, \quad (2)$$

or can be cut off without any appreciable effect on the observables. The pulse is assumed to have a finite duration T, i.e., the electric field $F(t)$ satisfies

$$F(t<0)=F(t>T)=0. \quad (3)$$

Let $x(t)$ and $v(t)=dx(t)/dt$ be a classical trajectory of the electron in the laser field,

$$\frac{d^2x(t)}{dt^2}=-F(t), \quad (4a)$$

$$x(t\leqslant 0)=v(t\leqslant 0)=0. \quad (4b)$$

One finds

$$v(t)=-\int_0^t F(t')dt', \quad x(t)=\int_0^t v(t')dt'. \quad (5)$$

The transformation to the KH frame is defined by [6,7]

$$x_{\mathrm{L}}=x_{\mathrm{KH}}+x(t), \quad (6a)$$

$$\psi_{\mathrm{L}}(x_{\mathrm{L}},t)=\exp\left(iv(t)x_{\mathrm{L}}-\frac{i}{2}\int_0^t v^2(t')dt'\right)\psi_{\mathrm{KH}}(x_{\mathrm{KH}},t). \quad (6b)$$

Note that there is no difference between the two frames for $t\leqslant 0$. Substituting this into Eq. (1), one obtains

$$i\frac{\partial\psi_{\mathrm{KH}}(x_{\mathrm{KH}},t)}{\partial t}=\left(-\frac{1}{2}\frac{\partial^2}{\partial x_{\mathrm{KH}}^2}+V(x_{\mathrm{KH}}+x(t))\right)\psi_{\mathrm{KH}}(x_{\mathrm{KH}},t). \quad (7)$$

Thus electron's dipole interaction with the laser field in the laboratory frame is represented by a quiver motion of the center of the atomic potential in the KH frame. The main advantage of the KH frame in the context of the SS expansion approach is that the KH potential $V(x_{\mathrm{KH}}+x(t))$ is localized in a finite interval of x_{KH}—the interaction region. Indeed, taking into account Eq. (2), it differs from zero only for $x_-\leqslant x_{\mathrm{KH}}\leqslant x_+$, where

$$x_-=-X+\min[x(t)], \quad x_+=X+\max[x(t)]. \quad (8)$$

Hence all interactions are exactly taken into account if the box used in the calculations covers this interval.

The wave function in the laboratory frame at the moment when the pulse is over, $\psi_{\mathrm{L}}(x_{\mathrm{L}},T)$, can be obtained from the solution to Eq. (7) using Eqs. (6). The observables can be calculated by projecting this function onto bound and scattering states of the atomic Hamiltonian. The results can be seen to depend crucially on the values of $x(T)$ and $v(T)$. For simplicity, in this paper we assume that the classical trajectory satisfies

$$x(T)=v(T)=0. \quad (9)$$

In this case, there is no difference between the laboratory and KH frames for $t\geqslant T$ too. Function $\psi_{\mathrm{L}}(x_{\mathrm{L}},T)$ up to a constant phase factor coincides with $\psi_{\mathrm{KH}}(x_{\mathrm{L}},T)$, therefore observables in the two frames also coincide. Formulas for the spectrum of ionized electrons given in the next section apply to this particular case; their generalization to arbitrary values of the parameters $x(T)$ and $v(T)$ meets no difficulties but is foregone.

B. Siegert-state expansion

Let us rewrite Eq. (7) as (the subscript KH is omitted from here on for brevity)

$$i\frac{\partial\psi(x,t)}{\partial t}=H(t)\psi(x,t), \quad (10)$$

where

$$H(t)=H+U(x,t), \quad (11)$$

$$H=-\frac{1}{2}\frac{\partial^2}{\partial x^2}+V(x), \quad (12)$$

$$U(x,t) = V(x + x(t)) - V(x). \tag{13}$$

Note that both the time-independent $V(x)$ and time-dependent $U(x,t)$ parts of the KH potential $V(x+x(t))$ vanish beyond the interval $x_- \leqslant x \leqslant x_+$. In addition, $U(x,t)$ vanishes for $t \leqslant 0$ and $t \geqslant T$. All this complies with the assumptions made in [11], thus the present problem is reduced to the one considered there. From this point we invoke the formulation developed in Ref. [11].

Our goal is to find the solution to Eq. (10) satisfying the initial condition

$$\psi(x,t)|_{t\leqslant 0} = \phi_0(x)e^{-iE_0 t}, \tag{14}$$

where E_0 and $\phi_0(x)$ represent a bound state of the atomic Hamiltonian (12). Let us introduce the function and derivative value operators at $x=x_0$,

$$\mathcal{F}(x_0) = \delta(x - x_0), \quad \mathcal{D}(x_0) = \delta(x - x_0)\frac{d}{dx}, \tag{15}$$

and a pseudodifferential operator

$$\hat{\lambda}_t = i\sqrt{2i\frac{\partial}{\partial t}}. \tag{16}$$

For a more detailed discussion of this operator see [10]. Following [11], we rewrite Eq. (10) in a matrix form,

$$\left[\hat{\lambda}_t - \begin{pmatrix} 0 & 1 \\ -2\tilde{H}(t) & \mathcal{F} \end{pmatrix}\right]\begin{pmatrix} \psi(x,t) \\ \tilde{\psi}(x,t) \end{pmatrix} = 0, \tag{17}$$

where $\tilde{H}(t)$ is a Hermitized Hamiltonian,

$$\tilde{H}(t) = H(t) + \frac{1}{2}[\mathcal{D}(x_+) - \mathcal{D}(x_-)], \tag{18}$$

and

$$\mathcal{F} = \mathcal{F}(x_-) + \mathcal{F}(x_+). \tag{19}$$

Note that the apparent dimension of the Hilbert space is doubled on the step from Eq. (10) to Eq. (17). This enables one to incorporate the outgoing-wave boundary conditions satisfied by the solution to Eqs. (10) and (14),

$$\left(\frac{\partial}{\partial x} \mp \hat{\lambda}_t\right)\psi(x,t)\bigg|_{x=x_\pm} = 0, \tag{20}$$

and consequently to eliminate the outer free-space regions, $x<x_-$ and $x>x_+$, from the consideration. The SSs defined by the atomic Hamiltonian (12) are the solutions to the eigenvalue problem

$$(H - E_n)\phi_n(x) = 0, \tag{21a}$$

$$\left(\frac{d}{dx} \mp ik_n\right)\phi_n(x)\bigg|_{x=x_\pm} = 0, \tag{21b}$$

where $E_n=k_n^2/2$. The solution to Eq. (17) in the interaction region $x_- \leqslant x \leqslant x_+$ can be sought in the form [11]

$$\begin{pmatrix} \psi(x,t) \\ \tilde{\psi}(x,t) \end{pmatrix} = \sum_n a_n(t)\begin{pmatrix} \phi_n(x) \\ ik_n\phi_n(x) \end{pmatrix}. \tag{22}$$

The coefficients $a_n(t)$ in this expansion satisfy [11]

$$a_n(t) = \delta_{n0}e^{-iE_0 t} + \frac{i}{k_n}\sum_m \int_0^t g(t-t';k_n)U_{nm}(t')a_m(t')dt', \tag{23}$$

where

$$U_{nm}(t) = \int_{x_-}^{x_+} \phi_n(x)U(x,t)\phi_m(x)dx, \tag{24}$$

and $g(t;k)$ is the retarded Green's function for the operator $\hat{\lambda}_t - ik$, see [10]. Thus the TDSE (10) is reduced to a set of coupled equations in time. We note that these equations, both in the integral Volterra form (23) and in a pseudodifferential form given in Ref. [11], have a "memory." To propagate the solution, one needs to keep and use all the information obtained on previous steps. The memory results from nonlocality of the driving operator $\hat{\lambda}_t$ in Eq. (17) and is a price for incorporating the continuum. This feature differs the SS expansion approach from other time-dependent close-coupling schemes in atomic physics.

When the pulse is over, the wave function can be conventionally expanded as [11]

$$\psi(x,T) = \sum_{n\in\{b\}} C_n\phi_n(x) + \int_0^\infty [C_-(k)\varphi_-(x,k) + C_+(k)\varphi_+(x,k)]\frac{dk}{2\pi}, \tag{25}$$

where the summation runs over the bound states of H, and $\varphi_\pm(x,k)$ are the scattering states of H satisfying outgoing-wave boundary conditions at $x\to\pm\infty$, respectively. The physical observables are defined by the coefficients C_n and $C_\pm(k)$. In this paper, we consider only the spectrum of the ionized electrons. The momentum distributions of the electrons ejected to the left $(-)$ and right $(+)$ are defined by

$$P_\pm(k) = |C_\pm(k)|^2. \tag{26}$$

They can be expressed in terms of the solutions to Eqs. (23) as [11]

$$P_\pm(k) = k^2\left|\sum_n \frac{A_n(E)}{k_n(k-k_n)}\phi_n(x_\pm)\right|^2, \tag{27}$$

where $E=k^2/2$ and

$$A_n(E) = \sum_m \int_0^T e^{iEt}U_{nm}(t)a_m(t)dt. \tag{28}$$

The energy spectrum of the electrons and the total probability of ionization are

$$P(E) = \frac{P_-(k) + P_+(k)}{2\pi k}, \quad P_{\text{ion}} = \int_0^\infty P(E)dE. \tag{29}$$

C. Implementation

The numerical implementation of our approach is the same as in Ref. [11]. The Siegert eigenvalue problem (21) is converted to an algebraic form by expanding the solutions in terms of a finite N-dimensional discrete variable representation basis constructed from Legendre polynomials [14]. This yields a set of $2N$ SPSs which are used as a basis in the expansion (22). Thus we obtain $2N$ coupled equations (23) which are solved by a method described in [10]. The solution of Eqs. (23) is the most time-consuming part. The calculation time scales as NM^2, where M is the number of time steps. In our calculations, it varied from several minutes to several hours for pulses of femtosecond to picosecond duration. Once the solution to Eqs. (23) is obtained, the calculation of spectra (27) is very fast. The representation of spectra in the form (27) does not bare any intrinsic limitation on the resolution, so one can easily scan the energy interval of interest to locate arbitrarily narrow structures. The upper boundary of the converged energy spectrum is limited by the dimension of the basis N, and with the present basis it rapidly grows with N. The results reported below are converged with respect to all numerical parameters. In general, the whole scheme is very robust and accurate, although a faster algorithm for solving Eqs. (23) is desirable.

III. CALCULATIONS OF ABOVE-THRESHOLD IONIZATION SPECTRA

Here, we apply our method to the calculations of ATI spectra [25]. First, we consider perturbative regime, to test the method and to resolve a problem met in the laboratory frame [11]. We then move on to much stronger laser pulses. Among various features, an interesting oscillating substructure is found in multiphoton ATI peaks for high laser frequencies in the stabilization regime. We analyze the underlying interference mechanism and formulate conditions under which the effect is expected to appear. We demonstrate the effect also by calculations for a model describing photodetachment of H^-.

A. Perturbative regime: The model of Ref. [11] revisited

In [11], a model atom described by the Eckart potential

$$V(x) = -\frac{15/8}{\cosh^2 x} \tag{30}$$

was considered. This system has two bound states with energies $E_0=-9/8$ and $E_1=-1/8$; the ground state is chosen to be the initial state. In one of the examples discussed, the electric field of the laser pulse is given by

$$F(t) = F_0 \sin^2(\pi t/T)\cos \omega t, \quad 0 \leqslant t \leqslant T, \tag{31}$$

where $F_0=0.1$, $T=200$, and $\omega=\pi$, hence $\omega T/2\pi=100$ is an integer. Substituting this into Eqs. (5), one can check that conditions (9) are fulfilled. The potential (30) can be safely cut off at $|x|=X=5$ [11]. For $F(t)$ given by Eq. (31) and $\omega T/2\pi \gg 1$, the classical trajectory satisfies

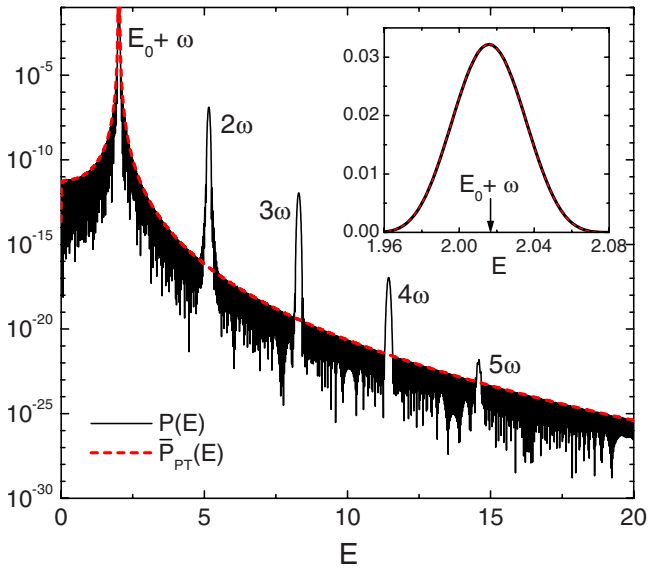

FIG. 1. (Color online) Present results for the model considered in Ref. [11], see Eqs. (30) and (31) with $F_0=0.1$, $T=200$, and $\omega=\pi$. One can clearly see a number of ATI peaks in the photoelectron spectrum $P(E)$ produced by multiphoton absorption from the ground state. For comparison, the envelope $\bar{P}_{PT}(E)$ of the perturbation theory results obtained by dropping the rapidly oscillating factor $\sin^2(ET/2)$ in Eq. (33) is also shown.

$$-\alpha \leqslant x(t) \leqslant \alpha, \quad \alpha = \frac{F_0}{\omega^2}. \tag{32}$$

Thus $x_\pm=\pm(X+\alpha)$, see Eqs. (8). For the above parameters we have $\alpha \approx 10^{-3}$, hence the interaction region $[x_-,x_+]$ in this case does not exceed the range of the potential $[-5,5]$.

The present results for this model are shown in Fig. 1. There are two differences compared to [11] to be mentioned here. First, some oscillations of the envelope of the background resulting from the cutoff of the laser field in the laboratory frame [11] no longer appear in the present approach. The KH frame takes the interaction with the laser field into full account, including that in the asymptotic region. Second, multiphoton peaks from the excited state are now buried in the background. Indeed, the probability of excitation in the present calculations is 1.96×10^{-12}, in close agreement with the result 1.95×10^{-12} of Ref. [11]. The height of the one-photon peak from the ground state is 3.1×10^{-2}, see Fig. 1, so that the height of the one-photon peak from the excited state is roughly estimated as $(1.96\times10^{-12})(3.1\times10^{-2}) \approx 6.1\times10^{-14}$, which falls well below visibility.

The above parameters of the laser pulse correspond to perturbative regime. To confirm the consistency of our approach, we compare our calculations with perturbation theory. The first-order perturbation theory result for the spectrum reads [7]

$$P_{\mathrm{PT}}(E) = |x(E-E_0)|^2 \frac{|d_-(k)|^2 + |d_+(k)|^2}{2\pi k}, \tag{33}$$

where

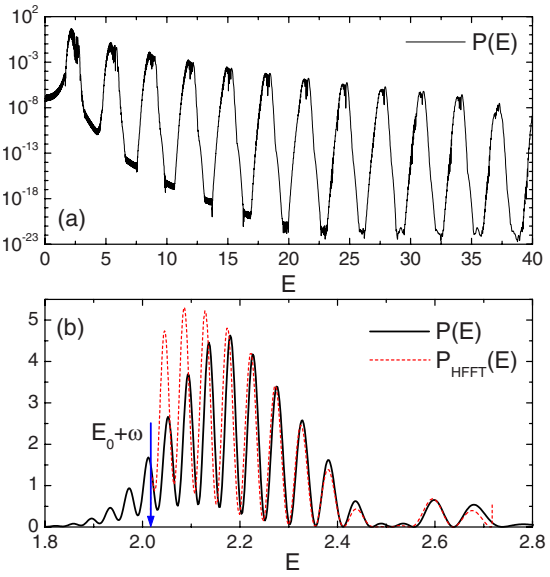

FIG. 2. (Color online) Photoelectron spectrum $P(E)$ for the same model as in Fig. 1, but for a very strong laser pulse with $F_0=30$. The lower panel enlarges the first ATI peak. Two bunches of oscillations can be seen at energies around $E(\alpha=\alpha_{c1})+\omega\approx 2.19$ and $E(\alpha=\alpha_{c2})+\omega\approx 2.62$, see text. $P_{\mathrm{HFFT}}(E)$ shows the results obtained from Eq. (43).

$$d_{\pm}(k)=\int \varphi_{\pm}^{*}(x,k)\frac{dV(x)}{dx}\phi_0(x)dx, \tag{34}$$

and $x(E)$ is the Fourier transform of the trajectory $x(t)$. Function $x(E)$ contains a rapidly oscillating factor $\sin(ET/2)$ [11]. In Fig. 1, for clarity, we show the perturbation theory results obtained by dropping this factor, even though our calculations reproduce it. There is a perfect agreement between the results in the one-photon peak as well as in the background; multiphoton peaks are beyond the first-order perturbation theory, of course.

B. Interference substructure of ATI peaks in the stabilization regime

Now, when the method has been tested, the physics in many different regimes can be analyzed. In this paper, we chose one particular cut of the parameter space where the laser frequency ω is larger than the ionization potential $|E_0|$. We wish to see what happens as the strength of the pulse grows. Let us consider the same model defined by Eqs. (30) and (31), again with $T=200$ and $\omega=\pi$. To illustrate our findings, we skip intermediate values of F_0 and proceed directly to a superstrong pulse with $F_0=30$ (a more realistic model is considered below). In this case $\alpha\approx 3$, see Eq. (32), hence the interaction region is $[x_-,x_+]=[-8,8]$, which is less than twice the range of the atomic potential. The spectrum of the ionized electrons for this model is shown in Fig. 2(a). One still can see a train of multiphoton peaks, although of a quite different shape as compared to the previous case. The first peak is enlarged in linear scale in Fig. 2(b). We note that $E_0+\omega\approx 2.017$ and $E_1+\omega\approx 3.017$ for the present parameters, so the spectrum in Fig. 2(b) is certainly produced by one-photon absorption from the ground state, however, it looks qualitatively different from the one-photon peak in Fig. 1. Higher-order ATI peaks have a similar oscillating substructure. Let us discuss its physical origin.

An adequate framework is provided by the high-frequency Floquet theory (HFFT) [8]. For a *monochromatic* laser field with the amplitude F_0 and frequency ω [one should simply drop the pulse envelope factor $\sin^2(\pi t/T)$ in Eq. (31)] the classical trajectory is $x(t)=\alpha\cos\omega t$ [the initial conditions (4b) become immaterial in this case]. Then the KH potential can be expanded into a Fourier series,

$$V(x+\alpha\cos\omega t)=\sum_{n=-\infty}^{\infty}V_n(x;\alpha)e^{-in\omega t}. \tag{35}$$

In the leading order of the HFFT, our model atom in the KH frame is described by [26]

$$\left(-\frac{1}{2}\frac{d^2}{dx^2}+V_0(x;\alpha)-E\right)\psi(x)=0. \tag{36}$$

It can be seen that the "dressed" potential $V_0(x;\alpha)$ coincides with $V(x)$ in the absence of the laser field, i.e., for $\alpha=0$. Let $E_0(\alpha)$ and $\phi_0(x;\alpha)$ be the bound-state solution to Eq. (36) which coincides with the initial state E_0 and $\phi_0(x)$ of the unperturbed atom for $\alpha=0$. The width of this state corresponding to the absorption of one photon is [27]

$$\Gamma(\alpha)=\frac{\Gamma_{-}(\alpha)+\Gamma_{+}(\alpha)}{2\pi k(\alpha)}, \tag{37}$$

where

$$\Gamma_{\pm}(\alpha)=2\pi\left|\int\varphi_{\pm}^{*}(x,k(\alpha);\alpha)V_1(x;\alpha)\phi_0(x;\alpha)dx\right|^2. \tag{38}$$

Here $k(\alpha)=\sqrt{2[E_0(\alpha)+\omega]}$ is the momentum of the ionized electron and $\varphi_{\pm}(x,k;\alpha)$ are the scattering-state solutions to Eq. (36) coinciding with $\varphi_{\pm}(x,k)$ for $\alpha=0$, see Eq. (25). Functions $E_0(\alpha)$ and $\Gamma(\alpha)$ for the present model are shown in Fig. 3(a). Their behavior is qualitatively similar to that calculated for a different model in Ref. [27].

In our case, the pulse is not monochromatic. However, its envelope is a slowly varying function (the pulse contains 100 optical cycles), so one could expect that the picture suggested by the HFFT will be followed adiabatically. The adiabatic approximation is implemented via the substitution

$$\alpha\to\alpha(t)=\frac{F_0}{\omega^2}\sin^2\frac{\pi t}{T}, \tag{39}$$

which makes the amplitude of the classical trajectory, see Eq. (32), a slow function of time. Functions $E_0(t)$ and $\Gamma(t)$ obtained from $E_0(\alpha)$ and $\Gamma(\alpha)$ upon such a substitution are shown in Fig. 3(b). These functions describe the energy and width of the initial atomic state "dressed" by the high-frequency laser field. Since $\Gamma(t)$ is small compared to $E_0(t)$, the dynamics can be approximately described as follows.

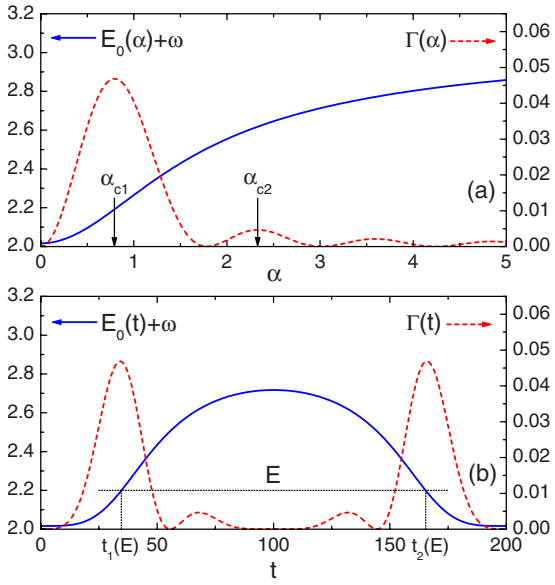

FIG. 3. (Color online) The energy and width of the initial atomic state "dressed" by the high-frequency laser field as functions of the amplitude α of classical trajectory and time t related to each other by Eq. (39) with $F_0/\omega^2 \approx 3$.

The probability for the atom to stay in the initial state until the moment t is

$$P_0(t) \approx \exp\left[-\int_0^t \Gamma(t')dt'\right]. \tag{40}$$

This gives $P_0(T) \approx 0.115$. Meanwhile, our accurate calculations yield the survival probability $P_0 = 0.126$ and ionization probability $P_{\text{ion}} = 0.874$, the probability of excitation $P_1 \approx 8 \times 10^{-8}$ being negligible. Thus the approximation (40) is actually not too bad. The key to understanding the dynamics is that under the adiabatic approximation there exists a relation between the energy E of a photoelectron and the moment t of its ionization,

$$E = E_0(t) + \omega \rightarrow t = t(E). \tag{41}$$

Because of this relation, the electrons ionized in the interval from t to $t+dt$ have energies between E and $E+dE$, where $E = E_0(t) + \omega$ and $dE = [dE_0(t)/dt]dt$. Equating the probability of ionization during this interval $P_0(t)\Gamma(t)dt$ to $C^2(E)|dE|$, where $C(E)$ is the amplitude of the wave packet created, we obtain

$$C(E) = \sqrt{P_0(t)\Gamma(t)\left|\frac{dt}{dE}\right|}\Bigg|_{t=t(E)}. \tag{42}$$

For the present pulse, $t(E)$ is a double-valued function: it has two branches, $t_1(E) \in [0, T/2]$ and $t_2(E) \in [T/2, T]$, corresponding to the rising and falling parts of the pulse, see Fig. 3(b). Hence there are two moments, $t_1(E)$ and $t_2(E)$, contributing to the spectrum at given energy E. Let $C_1(E)$ and $C_2(E)$ be the corresponding amplitudes defined by Eq. (42). The first wave packet created at $t_1(E)$ evolves between $t_1(E)$ and $t_2(E)$ with the energy E; the second wave packet created at $t_2(E)$ bears an additional phase accumulated between $t_1(E)$ and $t_2(E)$ by the bound state evolving with the energy $E_0(t) + \omega$. Taking these time-dependent phase factors into account, one obtains the spectrum of electrons produced by the absorption of one photon

$$P_{\text{HFFT}}(E) = |C_1(E) + C_2(E)e^{i\Phi(E)}|^2, \tag{43}$$

where the interference phase is given by

$$\Phi(E) = E[t_2(E) - t_1(E)] - \int_{t_1(E)}^{t_2(E)} [E_0(t) + \omega]dt. \tag{44}$$

Formula (43) can be easily generalized to the absorption of several photons as well as to the case when Eq. (41) has more than two solutions.

The results obtained using the above equations are shown in Fig. 2(b). In general, the adiabatic HFFT nicely reproduces the oscillating substructure of the first ATI peak. Some disagreement in the amplitude of the oscillations at lower energies is explained by the fact that the validity of HFFT requires $\omega \gg |E_0|$ and $\alpha^2(t)\omega \gg 1$ [26], but the second condition is not satisfied in the beginning and end of the pulse, where electrons with lower energies are produced. The main limitation of our approximate theory is that it accounts only for electrons with energies in a *finite* interval from $\min[E_0(t)] + \omega = E_0 + \omega$ to $\max[E_0(t)] + \omega$. The lower boundary of this interval is indicated by the arrow in Fig. 2(b); Eq. (43) diverges at the upper boundary because of the factor $dt(E)/dE$ in Eq. (42), which can be seen as a sharp rise of the curve $P_{\text{HFFT}}(E)$ at $E \approx 2.72$. A more accurate approximation free from this limitation could be developed, but this goes beyond the scope of the present paper.

Having demonstrated that the adiabatic HFFT is qualitatively correct, we now give a very rough picture of the dynamics explaining what happens with the first ATI peak as the amplitude of the pulse F_0 grows, while its frequency ω remains unchanged. This can be understood in terms of the behavior of $\Gamma(t)$, since the ionization dominantly occurs near the maxima of $\Gamma(t)$. If $\max[\alpha(t)] = F_0/\omega^2$ is smaller than the first critical value α_{c1} defined by the abscissa of the first maximum of $\Gamma(\alpha)$, $\alpha_{c1} \approx 0.79$ for the present model, then $\Gamma(t)$ has only one maximum at the maximum of the pulse, and only one wave packet is created. The spectrum in this case consists of a single peak located at $E = E(\alpha = F_0/\omega^2) + \omega$ with a rapidly decaying interference substructure in its *left* wing. If F_0/ω^2 becomes larger than α_{c1}, then function $\Gamma(t)$ has two maxima, one in the rising and one in the falling parts of the pulse, hence a pair of wave packets is created. In this case, the spectrum acquires quite a different shape: it consists of a peak located at $E = E(\alpha = \alpha_{c1}) + \omega \approx 2.19$ and modulated by the interference of the two wave packets, see Fig. 2(b). In the calculations shown in Fig. 2 we have $F_0/\omega^2 \approx 3$, which is larger than the second critical value $\alpha_{c2} \approx 2.33$, see Fig. 3(a). Function $\Gamma(t)$ in this case has totally four humps, see Fig. 3(b). The smaller ones produce a second pair of wave packets and result in an additional modulated peak in the spectrum at $E = E(\alpha = \alpha_{c2}) + \omega \approx 2.62$, see Fig. 2(b). More pairs of wave packets are created and more

peaks modulated by their interference appear in the spectrum as F_0/ω^2 becomes larger than higher maxima of $\Gamma(\alpha)$, if any. The number of fringes in each peak is determined by the interference phase (44) and grows proportionally to the length of the pulse T. Their contrast depends on the ratio of the amplitudes $C_1(E)$ and $C_2(E)$ in Eq. (43) and decays as T grows.

Summarizing, the conditions under which a pronounced interference substructure in ATI peaks is expected to appear can be formulated as follows: (a) $\omega \gg |E_0|$, (b) $F_0/\omega^2 > \alpha_{c1}$, and (c) T is not too small, to have at least a few fringes, and not too large, to have a good contrast. We note that the very existence of a maximum of function $\Gamma(\alpha)$ as well as conditions (a) and (b) are prerequisites for one of the scenarios of the phenomena of atomic stabilization [8,9]. Our analysis thus shows that under certain conditions on the length of the laser pulse ATI spectra produced in the stabilization regime should possess an interference substructure of the type discussed above.

Closing this section, we mention that an interference of wave packets created in the rising and falling parts of a laser pulse has been discussed in many different contexts. For example, an interference substructure in the *right* wing of ATI peaks was found in Ref. [5]. Some related interference effects in the excitation [28] and ionization [29] of atoms were observed experimentally. All such effects contain a phase which sometimes looks superficially similar to ours, Eq. (44). However, as far as we know, the interference mechanism in the stabilization regime we found has never been discussed in the literature.

IV. A MORE REALISTIC MODEL: PHOTODETACHMENT OF H^-

Let us show that our effect can be found in a more realistic situation. Consider a one-dimensional model of the negative hydrogen ion H^- described by the potential

$$V(x) = -24.856 \times \frac{\exp[-(x^2+4^2)^{1/2}]}{(x^2+6.27^2)^{1/2}}. \tag{45}$$

This model was used, e.g., in Ref. [30,31]. The potential (45) supports only one bound state with $E_0 \approx -0.0277$ (−0.754 eV), in close agreement with the binding energy of the real H^- ion. Our calculations show that this potential can be safely cut off at $|x|=X=15$, in agreement with [30]. Let the laser field be defined by Eq. (31) with $F_0=0.5$ ($I=cF_0^2/8\pi=8.8\times10^{15}$ W/cm^2), $\omega=\pi/10$ (8.55 eV), and $T=2000$ (48.4 fs), hence the pulse again contains $\omega T/2\pi=100$ optical cycles. Though somewhat speculative at present, a laser in this parameter range is expected to come into practical use in view of the recent experimental progress with free-electron lasers [32]. In this case $\alpha \approx 5$, see Eq. (32), so the interaction region is $[-20,20]$. We note that to generate a spectrum in [30] a huge box of the size 3276 was required. Our results for this model are shown in Fig. 4; they look similar to the results in Fig. 2. In the present case, the first maximum of $\Gamma(\alpha)$ occurs at $\alpha_{c1} \approx 2.32$, and at $\alpha \approx 5.25$ the function hits its first minimum. Hence only one pair of ionized electron wave packets is produced and only

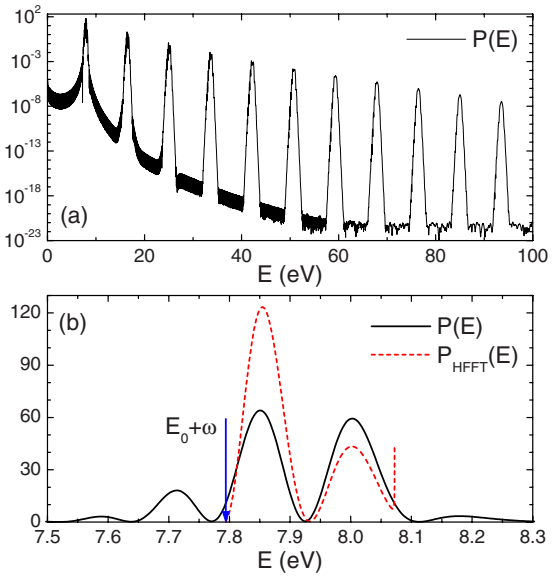

FIG. 4. (Color online) The spectrum $P(E)$ of electrons produced by irradiating a model one-dimensional ion H^- by a laser pulse with intensity $I=8.8\times10^{15}$ W/cm^2, photon energy $\hbar\omega=8.55$ eV, and duration $T=48.4$ fs (100 optical cycles). The total ionization probability is $P_{\text{ion}} \approx 0.45$. The lower panel enlarges the first ATI peak. $P_{\text{HFFT}}(E)$ shows the results obtained from Eq. (43).

one bunch of oscillations with the center at $E=E(\alpha=\alpha_{c1})+\omega \approx 0.29$ (7.90 eV) is seen in the first ATI peak. Interestingly, in Ref. [31] under slightly different conditions ($I=5\times10^{14}$ W/cm^2 and $\omega=2.5$ eV) a pair of wave packets were detected on the spatial distribution of the photoelectron probability density, see Fig. 3(b) there. It was argued that they are created in the rising and falling parts of the laser pulse, but the spectrum was not calculated. We think that was the first, even though indirect, observation of the mechanism as discussed above.

V. CONCLUSION

In this paper, we applied the Siegert-state expansion approach [10,11] to the solution of the TDSE describing a one-dimensional laser-atom interaction problem in the Kramers-Henneberger frame [6,7]. The main advantage of our method is that no unphysical reflection from the boundary of the box considered in the calculations occurs and the interaction with the laser field, including that in the asymptotic region, is fully taken into account. So, it is possible to accurately calculate the physical quantities using very restricted box size, even for long laser pulses. The method is demonstrated by calculations of ATI spectra for a number of model problems. We found an interference substructure of ATI peaks generated by strong high-frequency laser pulses in the stabilization regime. The physical mechanism of this effect is interpreted in terms of an adiabatic version of the high-frequency Floquet theory [8,26] and conditions favorable for its observation are formulated. A recent generalization of the theory of Siegert pseudostates to nonzero angular momenta [17] should make the extension of the present approach to the three-dimensional case possible.

ACKNOWLEDGMENTS

We thank O. V. Tikhonova for useful discussions and drawing our attention to Ref. [31]. K.T. is supported by Japan Society for the Promotion of Science (JSPS). This work was supported in part by Grants-in-Aid for Scientific Research (C) from the Ministry of Education, Culture, Sports, Science and Technology, Japan, and the 21st Century COE program on "Innovation in Coherent Optical Science," and by JSPS Bilateral joint program between the U.S. and Japan.

[1] K. C. Kulander, Phys. Rev. A **35**, 445 (1987).
[2] H. G. Muller, Laser Phys. **9**, 138 (1999).
[3] T. Morishita, Z. Chen, S. Watanabe, and C. D. Lin, Phys. Rev. A **75**, 023407 (2007).
[4] J. A. Pèrez-Hernàndez and L. Plaja, Phys. Rev. A **76**, 023829 (2007).
[5] V. C. Reed and K. Burnett, Phys. Rev. A **43**, 6217 (1991).
[6] H. A. Kramers, *Collected Scientific Papers* (North-Holland, Amsterdam, 1956), p. 272.
[7] W. C. Henneberger, Phys. Rev. Lett. **21**, 838 (1968).
[8] M. Gavrila, J. Phys. B **35**, R147 (2002).
[9] A. M. Popov, O. V. Tikhonova, and E. A. Volkova, J. Phys. B **36**, R125 (2003).
[10] O. I. Tolstikhin, Phys. Rev. A **73**, 062705 (2006).
[11] O. I. Tolstikhin, Phys. Rev. A **74**, 042719 (2006).
[12] A. J. F. Siegert, Phys. Rev. **56**, 750 (1939).
[13] O. I. Tolstikhin, V. N. Ostrovsky, and H. Nakamura, Phys. Rev. Lett. **79**, 2026 (1997).
[14] O. I. Tolstikhin, V. N. Ostrovsky, and H. Nakamura, Phys. Rev. A **58**, 2077 (1998).
[15] G. V. Sitnikov and O. I. Tolstikhin, Phys. Rev. A **67**, 032714 (2003).
[16] K. Toyota, T. Morishita, and S. Watanabe, Phys. Rev. A **72**, 062718 (2005).
[17] P. A. Batishchev and O. I. Tolstikhin, Phys. Rev. A **75**, 062704 (2007).
[18] O. I. Tolstikhin, I. Yu. Tolstikhina, and C. Namba, Phys. Rev. A **60**, 4673 (1999).
[19] K. Toyota and S. Watanabe, Phys. Rev. A **68**, 062504 (2003).
[20] G. V. Sitnikov and O. I. Tolstikhin, Phys. Rev. A **71**, 022708 (2005).
[21] S. Yoshida, S. Watanabe, C. O. Reinhold, and J. Burgdörfer, Phys. Rev. A **60**, 1113 (1999).
[22] S. Tanabe, S. Watanabe, N. Sato, M. Matsuzawa, S. Yoshida, C. O. Reinhold, and J. Burgdörfer, Phys. Rev. A **63**, 052721 (2001).
[23] R. Santra, J. M. Shainline, and C. H. Greene, Phys. Rev. A **71**, 032703 (2005).
[24] G. García-Calderón, J. L. Mateos, and M. Moshinsky, Phys. Rev. Lett. **74**, 337 (1995).
[25] P. Agostini, F. Fabre, G. Mainfray, G. Petite, and N. K. Rahman, Phys. Rev. Lett. **42**, 1127 (1979).
[26] M. Gavrila and J. Z. Kaminski, Phys. Rev. Lett. **52**, 613 (1984).
[27] M. Marinescu and M. Gavrila, Phys. Rev. A **53**, 2513 (1996).
[28] S. Yoakum, L. Sirko, and P. M. Koch, Phys. Rev. Lett. **69**, 1919 (1992).
[29] R. R. Jones, Phys. Rev. Lett. **74**, 1091 (1995).
[30] W. G. Greenwood and J. H. Eberly, Phys. Rev. A **43**, 525 (1991).
[31] A. M. Popov, O. V. Tikhonova, and E. A. Volkova, Laser Phys. **5**, 1184 (1995).
[32] V. Ayvazyan *et al.*, Eur. Phys. J. D **37**, 297 (2006).